PERGAMON

Journal of South American Earth Sciences 15 (2002) 157–171

Journal of
South American
Earth Sciences

www.elsevier.com/locate/jsames

Wide plate margin deformation, southern Central America and northwestern South America, CASA GPS observations

Robert Trenkamp[a,*], James N. Kellogg[a], Jeffrey T. Freymueller[b], Hector P. Mora[c]

[a]*Department of Geological Sciences, University of South Carolina, Columbia, SC 29208, USA*
[b]*Geophysical Institute, University of Alaska, Fairbanks, AK 99775, USA*
[c]*Volcanological and Seismological Observatory, INGEOMINAS, Avenida 12 de Octubre 15-47, Manizales, Colombia*

Received 1 November 2000; accepted 1 January 2002

Abstract

Global positioning system data from southern Central America and northwestern South America were collected during 1991, 1994, 1996, and 1998 in Costa Rica, Panama, Ecuador, Colombia, and Venezuela. These data reveal wide plate boundary deformation and escape tectonics occurring along an approximately 1400 km length of the North Andes, locking of the subducting Nazca plate and strain accumulation in the Ecuador–Colombia forearc, ongoing collision of the Panama arc and Colombia, and convergence of the Caribbean plate with Panama and South America. Elastic modeling of observed horizontal displacements in the Ecuador forearc is consistent with partial locking (50%) in the subduction zone and partial transfer of motion to the overriding South American plate. The deformation is hypothesized to reflect elastic recoverable strain accumulation associated with the historic seismicity of the area and active faulting associated with permanent shortening of 6 mm/a. Deformation associated with the Panama–Colombia collision is consistent with elastic strain accumulation on a fully locked Atrato–Uraba Fault Zone suture.

Keywords: GPS; North Andes; oblique subduction; arc continent collision; earthquake strain; escape; caribbean

1. Introduction

Mid-ocean ridge and transform fault azimuths, spreading rates, and earthquake slip vectors at plate boundaries have successfully explained large-scale features of plate kinematics and demonstrated that plate interiors generally behave rigidly over geologic time scales (Le Pichon, 1968; Minster et al., 1974; Minster and Jordan, 1978; Chase, 1978; DeMets et al., 1990). However, convergent plate boundaries were recognized early in the development of plate tectonics as wide zones of deformation, and those boundaries involving a continental plate boundary are much wider than are those consisting only of oceanic plates (Isaacs et al., 1968; Dewey and Bird, 1970; Freymueller et al., 1993; Kellogg and Vega, 1995; Gutscher et al., 1999). Global positioning system (GPS) measurements provide cost-effective and precise constraints on models of plate tectonic processes at convergent boundaries, such as continuum deformation versus microplate or block rotation (Thatcher, 1995).

The Central and South America (CASA) GPS project was inaugurated in 1988 to study plate motions and crustal deformation in a tectonically active area of complex interaction among the Nazca, Cocos, Caribbean, and South American plates (Fig. 1). The tectonic development of the CASA area has been the object of multiple geologic and geophysical studies (for a comprehensive listing, see Kellogg and Vega, 1995; Ego et al., 1996; Gutscher et al., 1999 and references therein). Previous studies have shown the CASA region to be a complex area of plate convergence and deformation, but the location of plate boundaries remains uncertain. At least two microplates, Panama and North Andes, have been hypothesized by Kellogg et al. (1985) and Kellogg and Vega (1995) (Figs. 1 and 2). This paper presents the results of CASA geodetic measurements spanning the years 1991–1998 in Costa Rica, Panama, Colombia, Ecuador, and Venezuela and focuses on GPS measurements related to the following:

1. Oblique subduction at the Ecuador trench and the 'escape'of the North Andes;
2. Earthquake strain accumulation at the Ecuador trench;
3. Island arc–continent collision, Panama–Colombia; and
4. Caribbean plate subduction.

* Corresponding author. Tel.: +1-803-777-4501; fax: +1-803-777-9133.
E-mail address: trenkamp@geol.sc.edu (R. Trenkamp).

0895-9811/02/$ - see front matter
PII: S0895-9811(02)00018-4

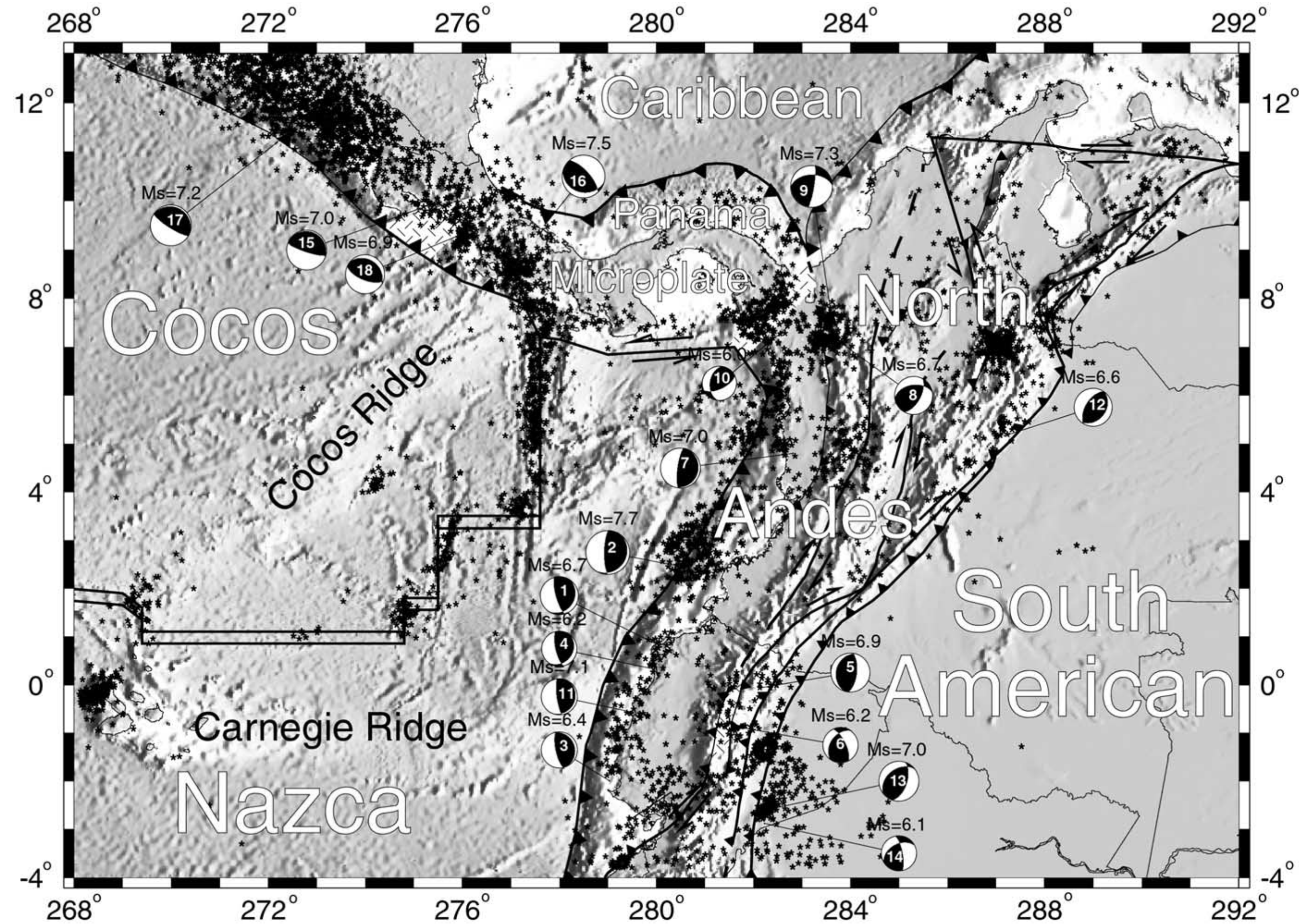

Fig. 1. Tectonic map for the CASA GPS project area. Seismicity with magnitudes greater than 4 between 1973 and 1999 (NEIC/USGS) are plotted with small black asterisks. Focal mechanisms (Harvard CMT) are plotted for major earthquakes with their magnitudes. The large earthquakes are referenced to Table 1 by the numbers superimposed on the compressional quadrant.

2. Data analysis

All data presented in this paper have been analyzed using GIPSY OASIS or GYPSY OASIS II software developed at the Jet Propulsion Laboratory (JPL), California Institute of Technology (Lichten and Border, 1987; Blewitt, 1989, 1990). Details of the 1991 data analysis are given in Freymueller (1991) and Freymueller et al. (1993). Each day of 1991 data was analyzed independently using GIPSY OASIS, the data from all stations in the CASA region, and data from tracking sites distributed over almost half the globe. The 1994, 1996, and 1998 data were analyzed using GIPSY OASIS II. All days were analyzed independently using all the stations in the CASA region and a tracking network similar in the number of stations to the 1991 campaign but with a more favorable regional geographic distribution for CASA due to the increased number of permanent sites, especially in the southern hemisphere. All the raw data were passed through automatic editors: Turboedit (Blewitt, 1990) for Rogue and Turborogue receivers and Phasedit (Freymueller, unpublished algorithm) for all other receivers. These editors find and correct cycle-slips (phase breaks in the data stream) and remove outliers. The data then are decimated to a 6-minute interval for data collected before 1996 and a 5-minute interval for data collected after 1996 to enable the use of the JPL's precise clocks and orbits. The GIPSY OASIS II solution suite of software was then run following a strategy similar to that described by Heflin et al. (1992) to obtain solutions based on all data available for a given day. All daily solutions, except those for 1991, were derived with weak constraints on initial positions and then transformed into ITRF96 using JPL-produced daily frame files. The 1991 data were transformed to ITRF96 using a seven-parameter transformation.

3. Velocity field descriptions

CASA GPS measurements used in this study were made during 1991, 1994, 1996, and 1998. Forty-four usable vectors for tectonic interpretation (Table 2, Fig. 3) were determined and are distributed over the major tectonic features of the study area. Two of our sites are located on

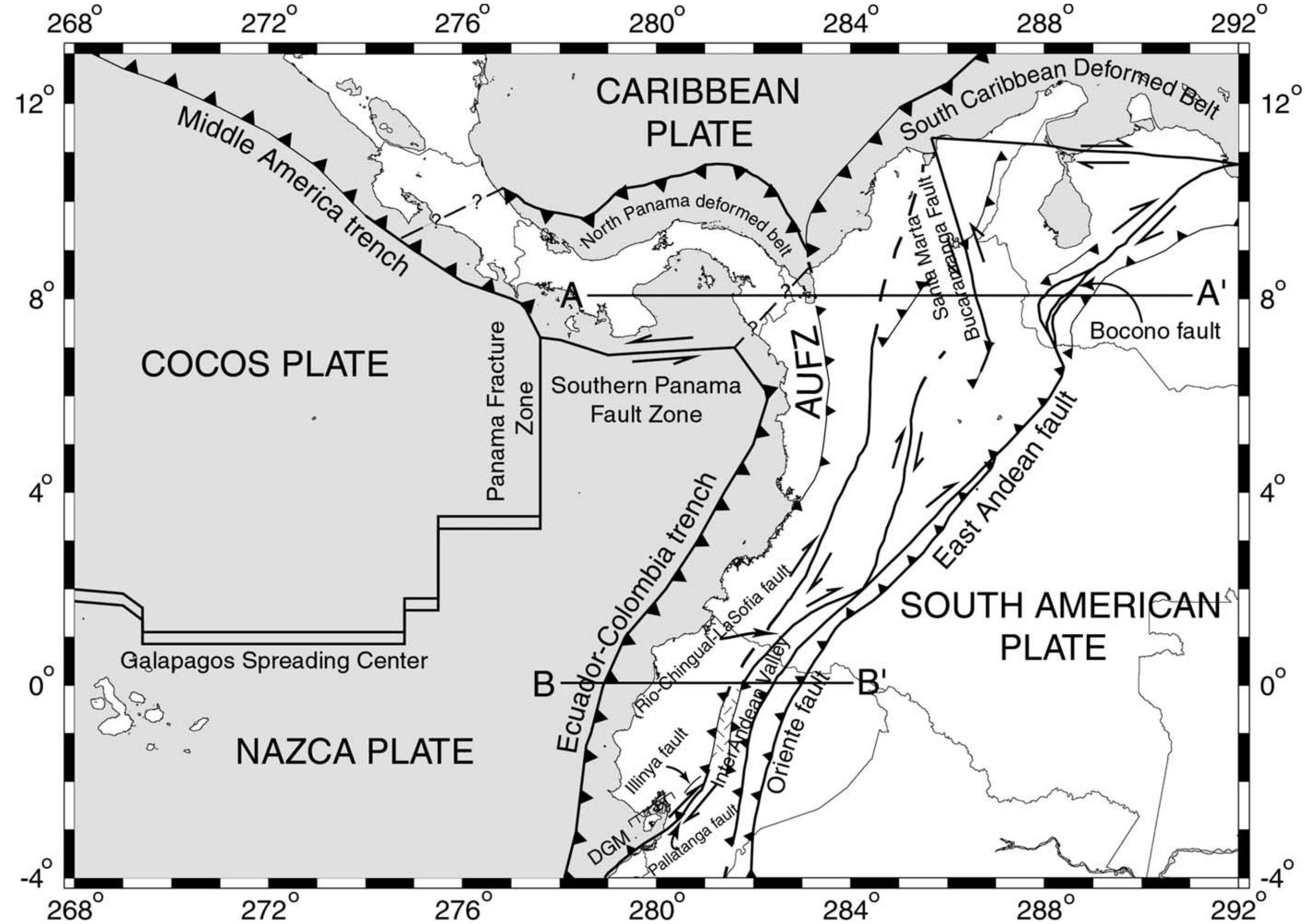

Fig. 2. Fault and tectonic feature map of the project area. A–A′ and B–B′ are the transects that were used for the modeling in Figs. 5 and 6.

the Nazca plate, the International GPS Service permanent station on the Galapagos Islands (GALA) and a station on Malpelo Island (MALS). The consistent velocities and directions for these two vectors indicate an approximately due east-oriented motion relative to a South America fixed reference frame (South America Euler pole and velocity in ITRF96; Edmundo Norabuena, personal communication, 2001) (Fig. 3).

East of the Colombia–Ecuador trench, the coastal stations MANT, PAJA, MUIS, ESME, and TUMA have vectors with a significant eastern component, though much smaller than the velocity vector measured for the subducting Nazca plate, whereas motions at the more northerly coastal sites, BUEN and BHSL, have a much smaller eastern component. The motion of the coastal sites suggests that some of the Nazca plate velocity is transferred directly to the overriding continental plate south of latitude 2°N. The velocity vectors of the more eastern stations in Ecuador and southern Colombia decrease eastward until measured velocities relative to stable South America are statistically not distinguishable from zero at LAGO, CONE, and VILL, east of the Eastern Andes frontal fault zone.

North and east of station TUMA, between latitudes 2°N and 6°N, the velocity vectors of the stations PAST, CALI, BUEN, MZAL, and BOGO have a distinctly greater northern component to their vectors. This suggests that the oblique component of the Nazca plate subduction is being accommodated by transpressive NE motion along faults subparallel to the Andean margin. Above latitude 6°N, stations RION, MONT, CART, BUCM, VDUP, and URIB have a greater eastward component to their velocity vectors, which is significant to at least 500 km from the trench and probably related to the ongoing Panama–Colombia collision (Kellogg and Vega, 1995). Stations VDUP and BUCM in Colombia, which are approximately 500 km from the collision zone, again show a significant northern component along with the eastern component. Stations ELBA and MERI in Venezuela, which are much farther from the Panama–Colombia collision zone, have similar vectors to those between 2°N and 6°N. Five station vectors in Panama, DAVI, CHIT, FLAM, ALBR, and CHEP, and three vectors in Costa Rica, LIMO, BRAT, and MANZ, give the relative magnitude and direction of the ongoing Panama–South America collision and imply relatively uniform translation of the Panama block. Two sites in western Costa Rica (LIBE and ETCG) have distinctly

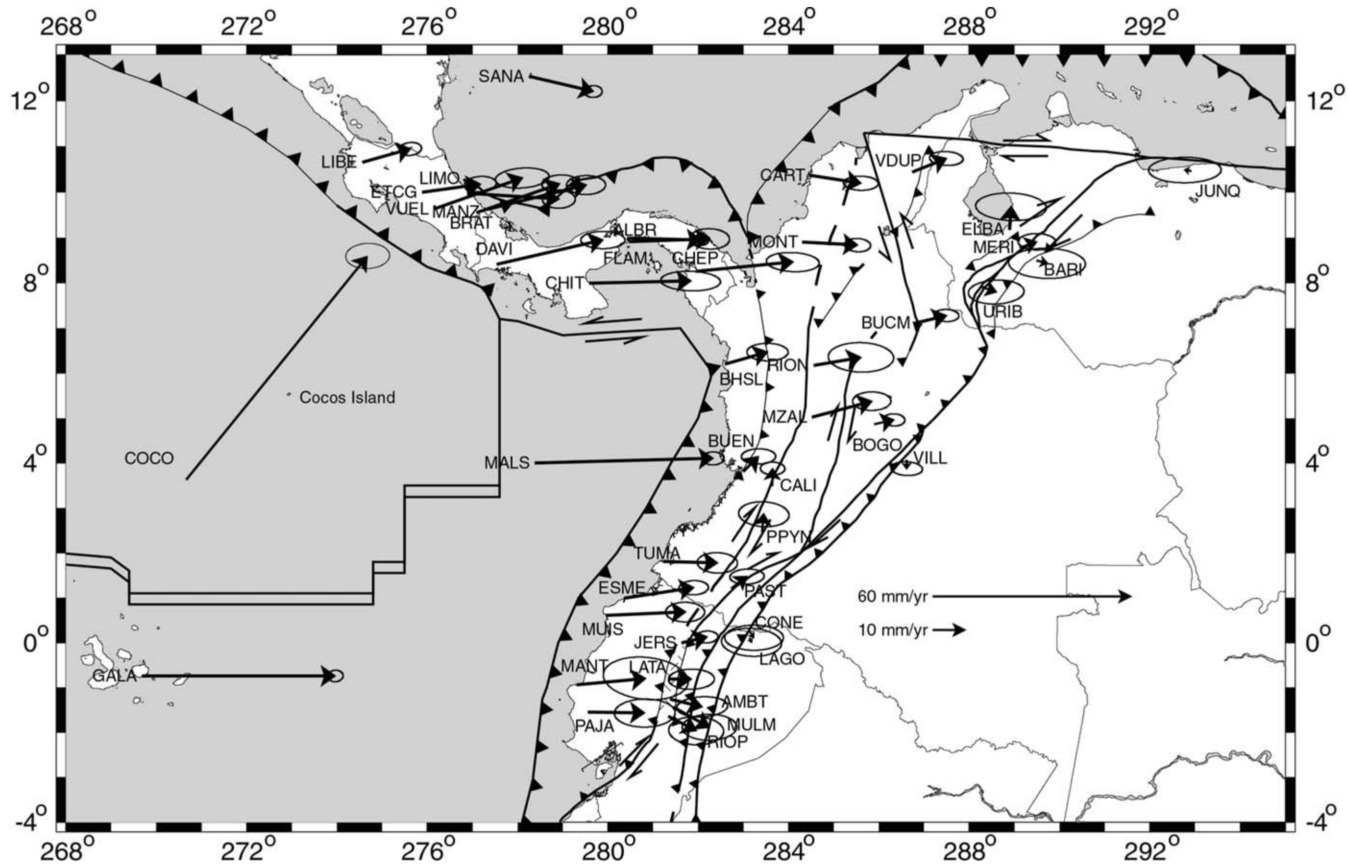

Fig. 3. Station velocity vectors relative to stable South America at 95% confidence using the data from the 1991, 1994, 1996, and 1998 CASA campaigns. The Cocos Island vector (COCO) was calculated relative to South America using a vector reported in Freymueller et al. (1993). Location of the COCO vector has been shifted to maintain the clarity of the figure.

different motions from those in eastern Costa Rica and Panama. These vectors provide some control on the western extent of the Panama microplate. The sole vector for the stable Caribbean plate, SANA, suggests continuing slow subduction of the Caribbean plate under northern Colombia and Panama.

4. Discussion

4.1. Oblique subduction at the Ecuador trench and escape of the North Andes

The North Andes Block is delineated by the Bocono fault, East Andean fault system and the Dolores Guayaquil megashear (DGM) to the east, the South Caribbean deformed belt on the north, and the Colombia–Ecuador trench and Panama on the west (Bowin, 1976; Pennington, 1981; Kellogg et al., 1985; Adamek et al., 1988; Ego et al., 1996; Gutscher et al., 1999) (Figs. 1 and 2). Schubert (1982) describes the Bocono fault in Venezuela as a right-lateral strike-slip fault that runs through the Merida Andes. Small-scale geodetic networks in the Merida Andes indicate compression normal to the Bocono fault, in addition to the strike-slip motion (Henneberg, 1983). Based on earthquake focal mechanisms Pennington (1981) proposes that transpressive right-lateral slip is occurring on the westward-dipping faults of the East Andean frontal fault system while the North Andes Block is moving NNE relative to the South American plate. The DGM is a system of northeast-trending, right-lateral strike-slip faults and north-trending thrust faults. Slip rates, based on morphology changes, along a splay of the Pallatanga fault in the central Ecuadorian Andes are reported as 3–4.5 mm/a (Winter et al., 1993). Seismic activity of the Iliniza fault, which is subparallel to and approximately 70 km to the north of the Pallatanga fault, is similar to that of the Pallatanga fault and probably has a similar slip rate (Hugo Yepes, Escuela Politecnica Nacional, Ecuador, personal communication, 1991). Slip rates are estimated as 7 ± 3 mm/a along the Rio–Chingual–La Sofia fault at the Ecuador–Colombia border, on the basis of offsets of dated pyroclastic flows (Ego et al., 1996). Tibaldi and Leon (2000) estimate a right-lateral displacement rate of 15–16 mm/a in northern Ecuador and 13 mm/a in southern Colombia using morphological offsets across several faults that correspond to the East Andean Frontal fault system. Earthquake slip rate estimates, offset glacial moraines, and Quaternary fault morphology suggest

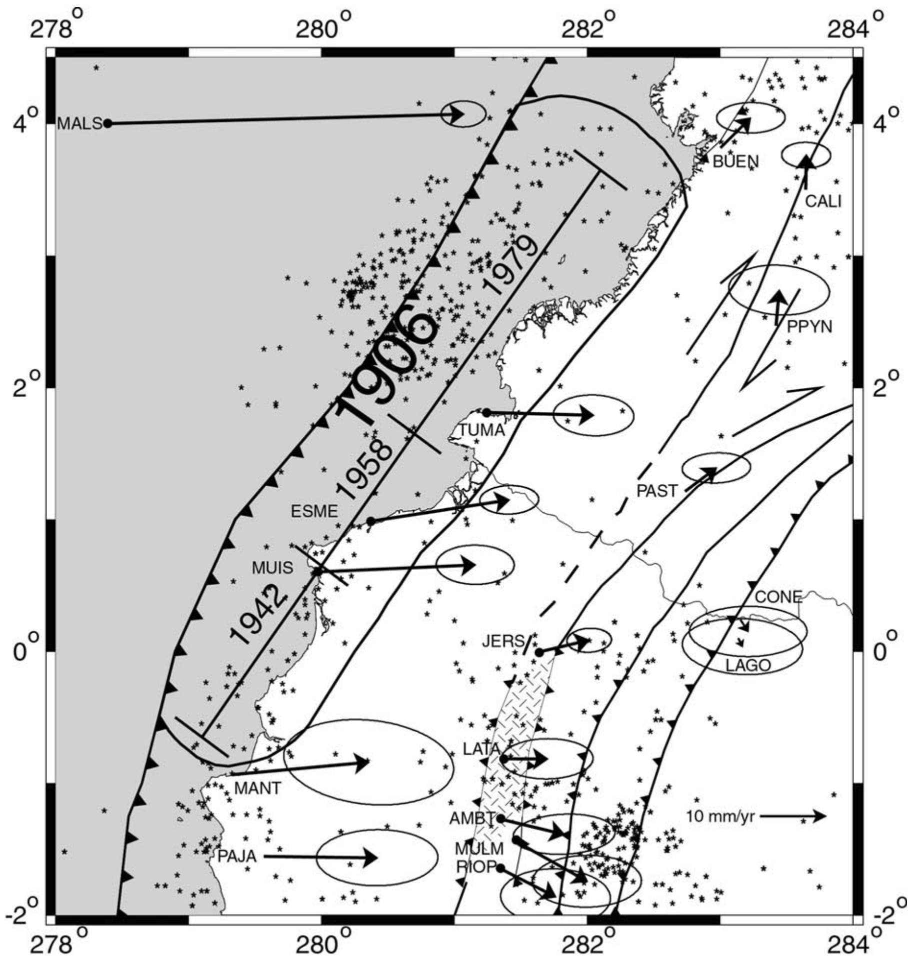

Fig. 4. Observed vectors relative to South America in the area of the great 1906 earthquake, which ruptured an over 500 km-long segment of the Colombia–Ecuador forearc. The 1942, 1958, and 1979 earthquake sequence reruptured the 1906 rupture zone. Rupture zones shown are after Kanamori and McNally (1982).

that the northern Andes are moving northeastward relative to stable South America at 4–10 mm/a along the Bocono fault in the Merida Andes of Venezuela (Schubert, 1980, 1982; Aggarwal, 1983; Lavenu et al., 1995).

CASA GPS measurements are consistent with rapid subduction of the Nazca plate and Carnegie aseismic ridge at the Ecuador trench beneath stable South America and show that the direction of this motion is oblique to the Colombia–Ecuador margin. As a result, the Andean margin is undergoing shortening perpendicular to the margin, and as predicted, the North Andes Block appears to be ‘escaping’ to the northeast parallel to the margin (Jarrard, 1986; Beck, 1991; McCaffrey, 1992). Relative to station BOGO, seven stations in the North Andes—LATA, JERS, PAST, BUEN, BUCM, URIB, and MERI—have statistically zero motion at two sigma. The velocity at BOGO relative to South America (6 ± 2 mm/a) is therefore interpreted as approximating the velocity of the North Andes Block relative to stable South America. This rate is less than the average North Andes–South America transcurrent motion rate for the Pleistocene, as measured by surficial geomorphic observations (Tibaldi and Leon, 2000). This slowing may be related to the slowing Nazca–South America subduction rates during the same period of time (Norabuena et al., 1999).

Transition of the boundary of the North Andes Block from the DGM in the south to the East Andean Frontal Fault system takes place on faults in and to the north of the Inter-Andean Valley (Lavenu et al., 1995; Ego et al., 1996; Gutscher et al., 1999). Four CASA sites (JERS, LATA, AMBT, and RIOP) are located from north to south within this transition zone. The measured velocity vectors rotate clockwise from north to south (Fig. 4). These motions are interpreted to indicate distributed right-lateral motion along a fault zone between RIOB and JERS or elastic deformation from a single locked fault.

The large eastern component of motion at sites in this transition zone is hypothesized to be due to permanent shortening related to the East Andean Frontal Fault system. The residual motions of other sites on the North Andes Block, which indicate deviations from coherent rigid plate behavior, are discussed in detail later.

Table 1
Summary information for the major earthquakes shown in Figs. 1 and 4 (source 1: Harvard CMT solution 2000; source 2: Kanamori and McNally (1982))

	Date	Longitude (degrees)	Latitude (degrees)	Depth (km)	M_o (10^{20} Nm)	M_s	Source
North Andes earthquakes							
	01/31/06	279.00	−0.75	25.0	20,000.00	8.7	2
	05/14/42	280.00	1.37	25.0	320.00	7.9	2
	01/19/58	280.60	1.00	60.0	520.00	7.8	2
1	04/09/76	280.11	0.79	19.4	11.10	6.7	1
2	12/12/79	281.19	2.32	19.7	1,690.00	7.7	1
3	05/06/81	279.03	−1.99	17.4	5.60	6.4	1
4	11/22/83	280.01	0.31	35.2	16.60	6.2	1
5	03/06/87	282.16	−0.06	15.0	63.70	6.9	1
6	09/22/87	281.74	−0.89	15.0	4.07	6.2	1
7	11/19/91	282.82	4.80	19.1	73.20	7.0	1
8	10/17/92	283.61	7.22	15.0	11.30	6.7	1
9	10/18/92	283.66	7.27	15.0	57.10	7.3	1
10	11/04/96	282.79	7.47	15.0	3.05	6.0	1
11	08/04/98	279.52	−0.57	25.6	63.70	7.1	1
East Andean Frontal Fault earthquakes							
12	01/19/95	287.17	5.16	16.0	7.07	6.6	1
13	10/03/95	282.47	−2.55	25.0	39.10	7.0	1
14	10/03/95	282.23	−2.88	15.0	5.38	6.1	1
Costa Rican earthquakes							
15	03/25/90	275.42	9.95	17.9	110.00	7.0	1
16	04/22/91	277.23	10.10	15.0	331.00	7.5	1
17	02/09/92	272.19	11.20	15.0	340.00	7.2	1
18	08/20/99	275.90	9.28	24.0	26.00	6.9	1

4.2. Earthquake strain accumulation at the Ecuador trench

Rapid subduction of the oceanic Nazca plate and aseismic Carnegie ridge (Fig. 3) (58 ± 2 mm/a) is occurring at the Colombia–Ecuador trench. The forearc north of the Carnegie ridge is historically seismically active (Kelleher, 1972; Kanamori and McNally, 1982; Mendoza and Dewey, 1984; Ruff, 1996; Swenson and Beck, 1996). During the 20th century, a sequence of four great ($M_s > 7.5$), subduction-related earthquakes occurred. The first and largest event of this series occurred in 1906 ($M_w = 8.8$) and, according to intensity reports and strong macroseismic activity, had a rupture length of 500 km (Kelleher, 1972; Kanamori and McNally, 1982). Kanamori and McNally (1982), using aftershock sequences to determine rupture areas, find that three smaller events in 1942 ($M_w = 7.9$), 1958 ($M_w = 7.8$), and 1979 ($M_w = 8.2$) appear to have reruptured most of the thrust fault plate boundary segment that ruptured during the 1906 event. However, the total of the seismic moments of the three events was barely 15% of the moment release during the 1906 event (Table 1) (Kanamori and McNally, 1982; Mendoza and Dewey, 1984). Nishenko (1989), studying earthquake zones on the Pacific Rim, estimated a 60–90% time-dependent probability for the recurrence of either a large ($7.0 < M_s < 7.7$) or great ($M_s > 7.7$) shallow-plate boundary earthquake during the 10-year period 1989–1999, and Papadimitriou (1993), studying only segments along the western coast of South and Central America and using a time-predictable model, gave a 68% time-dependent probability for a large ($M_s > 7.5$) earthquake in the same area during the 10-year period ending in 2002.

Several sites of the CASA network are well situated to measure the strain release in the event of a large earthquake in the area of the 1906 rupture zone and, more important, the strain that must be accumulating that would be capable of producing such an event. Three CASA vectors at sites near the coast at the Ecuador–Colombia border, at Muisne (MUIS) and Esmeraldas (ESME) in Ecuador and Tumaco (TUMA) in Colombia, have large east–northeast motion relative to stable South America (Figs. 3 and 4). Motion at the two sites in Ecuador average 21 mm/a relative to South America, whereas motion at the more northerly site in Colombia is 15 mm/a relative to South America. Differences in the rates at these three sites are probably purely related to distance from the trench, as all are within the rupture zone of the 1906 earthquake. The direction of the movement of these sites relative to stable South America is consistent with the direction of the subducting Nazca plate and Carnegie ridge, but the vectors have a smaller magnitude, which suggests that the motion reflects the partial transfer of motion of the subducting slab to the overriding continental plate. We hypothesize that the velocities of these coastal sites relative to South America reflect two modes of deformation approximately parallel to the direction of Nazca–South America convergence:

1. Deformation due to elastic recoverable strain accumulation associated with the seismic cycle at a locked or partially locked subduction zone interface, and

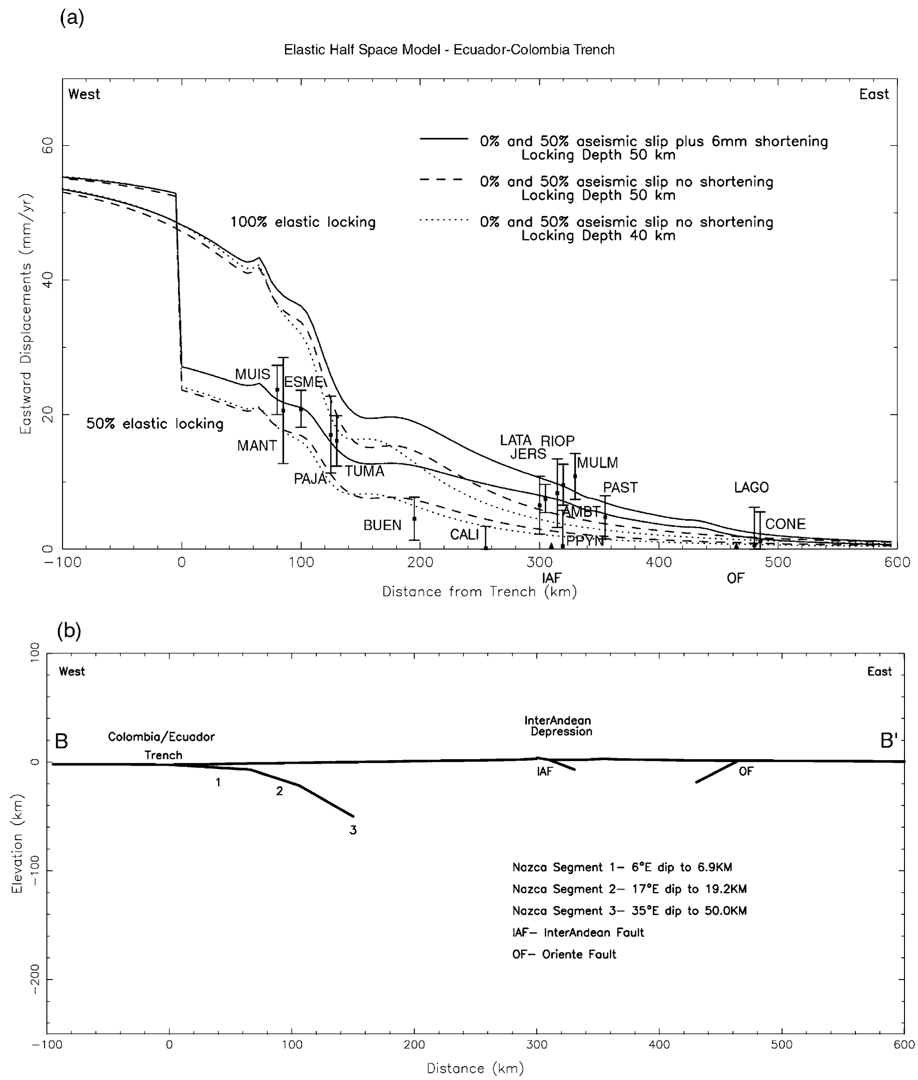

Fig. 5. a. CASA geodetic data at one standard error compared with elastic half-space models. A convergence rate of 58 mm/a was determined by repeat measurements of the Galapagos site (GALA). Shortening is modeled as 6 mm/a distributed as 3 mm/a on an east-dipping Inter-Andean fault (IAF) and 3 mm/a on a generalized west-dipping thrust (OF) in the Oriente Basin. The IAF dips at about 20° to the east and is assumed locked from 0 to 10 km depth (Lavenu et al., 1995). The modeled eastern thrust fault dips at 30° to the west and is locked from 0 to 20 km depth. Aseismic slip refers to that percentage of the slip accommodated aseismically at the subduction zone. b. Fault model for cross section B–B′. Line is located in Fig. 2.

2. Motion due to permanent shortening associated with active faulting in the Inter-Andean and East Andean frontal fault systems several hundred kilometers east of the subduction zone.

To test this hypothesis, the elastic strain in northern Ecuador and southern Colombia due to a locked subduction zone along the Colombia–Ecuador trench can be estimated using an elastic half-space model for a locked dipping thrust fault (Savage, 1983). The estimation of the dip related to the locked seismic zone (Fig. 5b) is based on seismicity (Pennington, 1981) and gravity and seismic refraction models (Meissner et al., 1976; Kellogg and Vega, 1995). Maximum locking depths are estimated at 40 km for the 1942, 1958, and 1979 earthquakes and at 50 km for the 1906 earthquake, following those determined by Kelleher (1972) and Kanamori and McNally (1982). Tichelaar and Ruff (1991) estimated similar locking depths (36–53 km) for subduction zones in the central and southern Andes.

Combining the approach of Savage (1983) with a boundary element modeling program (3D-DEF; Gomberg and Ellis, 1994), eastward surface strain is modeled by imposing back slip on a velocity field defined by the plate convergence, similar to the approach outlined by Leffler et al. (1997). The rate determined by the CASA project at GALA (58 mm/a) is used to simulate the locked segment. Various models with 40 and 50 km locking depths were run to compare models in which the entire east–west convergence is accommodated on the locked subduction interface (0% aseismic slip), models in which part of the slip on the subduction interface is accommodated aseismically (partial

Table 2
CASA vectors relative to South America fixed reference frame, showing east and north components with one sigma errors

Site	Longitude	Latitude	East (mm/a)	North (mm/a)	σ(E) (mm/a)	σ(N) (mm/a)
ALBR	280.44	8.99	22.06	−0.57	1.49	1.02
AMBT	281.35	−1.26	9.46	−2.28	3.14	1.24
BARI	289.50	8.48	3.08	−0.74	7.17	2.82
BHSL	282.61	6.20	12.67	3.62	3.85	1.64
BOGO	285.92	4.87	5.78	1.29	1.99	1.14
BRAT	277.11	9.55	24.99	8.69	3.43	1.62
BUCM	286.82	7.12	9.27	2.22	2.32	1.14
BUEN	283.01	3.82	4.51	4.49	3.20	1.42
CALI	283.64	3.50	0.08	5.13	2.29	1.20
CART	284.50	10.36	15.10	−2.34	3.24	1.32
CHEP	281.96	8.25	29.04	2.83	4.94	1.79
CHIT	279.59	7.99	30.48	0.69	5.58	1.83
CONE	283.15	0.24	1.12	−1.72	5.49	2.35
DAVI	277.56	8.41	31.80	7.33	4.12	1.61
ELBA	288.89	9.18	0.48	6.85	6.59	2.58
ESME	280.37	0.99	20.83	3.20	2.74	1.33
ETCG	275.89	10.00	17.49	2.41	2.97	1.44
FLAM	280.48	8.91	24.20	0.86	3.70	1.91
GALA	269.70	−0.74	58.18	−0.01	1.44	1.08
JERS	281.64	−0.01	7.48	1.78	2.08	1.12
JUNQ	292.91	10.46	−1.78	0.31	6.78	2.38
LAGO	283.14	0.10	0.59	−1.20	5.61	2.62
LATA	281.37	−0.81	6.51	−0.03	4.29	1.88
LIBE	274.57	10.65	14.32	4.05	2.09	1.21
LIMO	276.97	9.96	26.43	−1.66	3.08	1.70
MALS	278.39	4.00	53.62	1.43	2.09	1.21
MANT	279.33	−0.94	20.58	1.88	7.93	3.99
MANZ	277.32	9.62	29.86	7.38	3.65	1.77
MERI	289.13	8.79	4.99	1.66	3.50	1.53
MONT	284.32	8.89	16.51	−0.86	2.43	1.24
MUIS	279.98	0.60	23.65	1.06	3.64	1.83
MULM	281.46	−1.44	10.84	−6.09	5.09	2.43
MZAL	284.53	5.03	17.92	4.75	3.58	1.73
PAJA	279.57	−1.55	16.98	−0.23	5.67	2.62
PAST	282.74	1.22	4.68	3.51	3.20	1.41
PPYN	283.42	2.48	0.47	5.25	4.70	2.33
RION	284.57	6.18	14.09	2.38	6.11	2.76
RIOP	281.35	−1.65	8.28	−4.24	5.12	2.64
SANA	278.27	12.52	19.18	−4.49	1.65	1.11
TUMA	281.25	1.81	16.08	−0.42	3.76	1.91
URIB	288.26	7.91	4.66	−1.58	5.20	2.24
VDUP	286.75	10.44	10.10	4.02	3.14	1.30
VILL	286.62	4.07	0.00	−2.53	2.94	1.29
VUEL	276.15	9.62	26.64	9.38	5.02	1.88

decoupling), and models in which some of the convergence is accommodated on thrust faults within and east of the Andes mountains (Figs. 2 and 5) (Lavenu et al., 1995).

The CASA stations were projected parallel to the trench, to the east–west profile (B–B′, Fig. 2), so that the east–west distances between trench and stations were conserved. Shortening was modeled as 6 mm/a distributed as 3 mm/a on an east-dipping fault (IAF) within the Inter-Andean depression, approximately 320 km from the trench, dipping at 18°E, and locked from 0 to 10 km, and on a generalized west-dipping thrust (OF) in the Oriente Basin dipping 30°W and locked from 0 to 20 km (Fig. 5b).

The range of realistic locking depths seems to have a minimal effect on the model results. Fully locked models (0% aseismic slip) overestimate the GPS observations in the near trench stations. Models without permanent shortening underestimate the GPS observations for the eastern stations. A model with 50% locking (29 mm/a) plus 6 mm/a shortening on the eastern faults fits most of the observations well at 1 sigma confidence (Fig. 5a). These results are similar to those obtained by Norabuena et al. (1998) for the central Andes of Peru and Bolivia, who measured approximately 30–40 mm/a of locking and 10–15 mm/a of crustal shortening at the sub-Andean foreland fold and thrust belt. At the northern end of the 1906 rupture zone (Fig. 4), no significant locking is required to explain the motions of Buenaventura (BUEN), Cali (CALI), and Popayan (PPYN), Colombia (Fig. 5a).

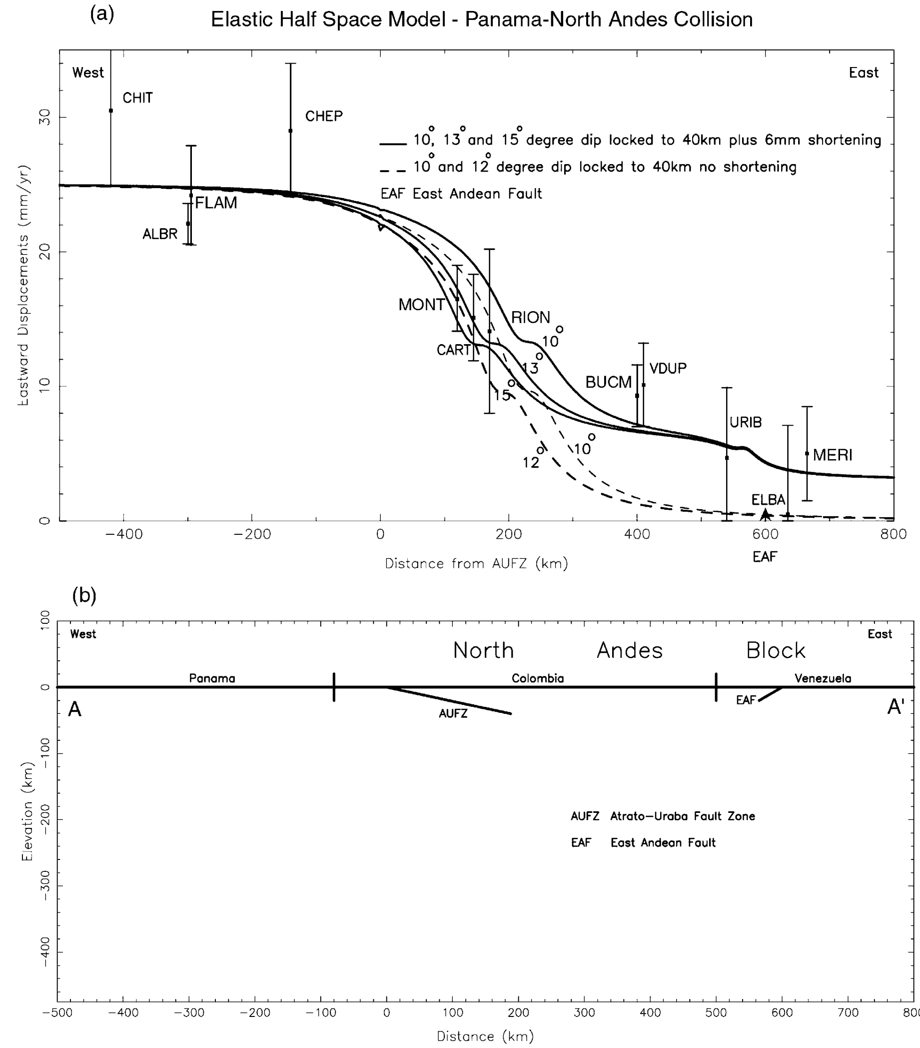

Fig. 6. a. CASA geodetic data at one standard error compared with elastic half-space models with various shallow dip angles on the AUFZ. The 25 mm/a Panama–South America convergence rate was determined using the average of four stations from the relatively aseismic stable Panama: CHIT, ALBR, FLAM, and CHEP. The displacement includes 3 mm/a shortening on a generalized thrust fault in the EAF system and 3 mm/a eastward component of the strike-slip motion associated with the escape of the North Andes Block. b. East–west cross section A–A′ of the collisional zone. Profile location is shown in Fig. 2.

Our shortening estimate (6 mm/a) is higher than the slow rate of Andean shortening inferred from seismic data (1.4–2.1 mm/a) by Suarez et al. (1983). The seismic estimate does not include aseismic deformation, and the sampling period may have missed infrequent, very large earthquakes. The observed strain accumulation and time since the last great earthquake in the region support the high conditional probability of a large or great earthquake in the near future (Nishenko, 1989; Papadimitriou, 1993). Assuming a 50% locked plate interface since the last large earthquake on the southern rupture zone in 1942, seismic slip has accumulated at a rate of approximately 29 mm/a for a total of 1.7 m. If the accumulated slip is released as a single event, the expected magnitude would be $M_w = 7.5 - 7.7$, using empirical scaling relations (Kanamori, 1983), which would be similar to the 1942 or 1958 events but smaller than the 1979 event.

4.3. Island arc–continent collision, Panama–Colombia

Panama and northern Colombia provide a unique opportunity to study the kinematics and mechanics of an active island arc–continent collision zone. The timing of the initial collision of Panama with northern Colombia is not well constrained, and different models span an interval of time from 12 to 20 Ma (Lonsdale and Klitgord, 1978; Keigwin, 1978, 1982; Wadge and Burke, 1983; Keller et al., 1989; Duque-Caro, 1990; Kellogg and Vega, 1995). The Panama–Colombia border area is a tectonically complex region that lies between the North Panama Deformed Belt and the Colombia–Ecuador trench (Fig. 2) in which more than 60 earthquakes of magnitude 5.0 or larger occurred between 1963 and 1981. Studies of seismicity in the border region and offshore suggest that east–west compression has produced an area of diffuse and complex faulting along northwest-to-northeast-trending strike-slip and thrust faults (Pennington, 1981; Adamek et al., 1988).

On October 17 and 18, 1992, a deadly sequence of two large shallow crustal earthquakes ($M_s = 6.6$ and $M_s = 7.3$) occurred near Murindo in northwestern Colombia (Table 2 and Fig. 1, #8–9). The 'best' fitting focal mechanism for the smaller event was a northeast-trending thrust event, whereas the larger event was associated with strike-slip motion on an inferred north-trending fault (Li and Toksoz, 1993; Wallace and Beck, 1993; Ammon et al., 1994). These focal mechanisms are consistent with compression normal to the Panama–North Andes suture (Freymueller et al., 1993).

Evidence for active Panama–North Andes collision was first reported by Kellogg and Vega (1995), and estimates of the total shortening exceed 150 km (Colletta et al., 1990). Relative to a fixed South America reference frame, four well-determined vectors in Panama (CHIT, ALBR, FLAM, and CHEP) demonstrate the ongoing collision of the Panama microplate with the North Andes Block at an average of 25 mm/a. The large eastern components of the vectors in northern Colombia (CART, MONT, RION, VDUP, and BUCM) suggest the transfer of motion from the Panama microplate collision. In the ongoing collision, the mechanical behavior of the Panama arc can be approximated as a rigid indenter. The wide continental plate boundary zone in Colombia appears to be compressing normal to the suture zone at the Panama–Colombia boundary. Monteria (MONT) (Fig. 3), 120 km east of the suture, is moving eastward at 16 ± 3 mm/a. The deformation appears to extend up to 600 km from the suture into the continental crust.

Deformation in northern Colombia due to the Panama collision can also be approximated by elastic half-space models for a locked dipping thrust fault (Savage, 1983; Gomberg and Ellis, 1994). An estimated maximum locking depth of 40 km is based on microseismicity studies near the Panama–Colombia suture zone that determined changes in focal mechanisms at approximately 36 km, coincident with the crust mantle boundary (Hutchings et al., 1981). All models assume that the entire east–west convergence is accommodated on the locked interface (no aseismic slip) at the Atrato–Uraba Fault Zone (AUFZ) (A–A′, Figs. 2 and 6b). Shortening is estimated as 3 mm/a locking on thrust faults in the East Andean Frontal fault (EAF) system and 3 mm/a through-going displacement of the strike-slip motion associated with the northward-directed escape of the North Andes Block.

Models without shortening do not fit the observed eastward displacements of BUCM, VDUP, and URIB (Fig. 6a). To model the motion observed at URIB, permanent shortening and northeastward escape on eastern faults are estimated to be about 6 mm/a. Near field sites MONT, CART, and RION are well modeled by a locked low-angle (13–15° thrust fault (AUFZ). The Valedupar (VDUP) and Bucaramanga (BUCM) vectors are not well matched by the models but may reflect unmodeled deformation produced by the Panama collision and Caribbean oblique subduction.

Proposed models for crustal deformation within Panama include a flexural beam (Silver et al., 1990), distributed left-lateral slip (Mann and Corrigan, 1990), a diffuse plate boundary accommodating deformation over a broad area (Jordan, 1975; Wadge and Burke, 1983), and the interaction of rigid microplates (Pennington, 1981; Adamek et al., 1988; Kellogg et al., 1989; Kellogg and Vega, 1995).

Relative to ALBR, vectors in Panama suggest that the central, virtually aseismic section of Panama (Figs. 1 and 3) is moving rigidly, whereas the DAVI vector in western Panama shows a northeast velocity. The vector at DAVI can be explained as elastic strain accumulation from the locked subduction of the Cocos Ridge under Central America (Lundgren et al., 1999).

Seismicity and GPS measurements in Panama and northern Colombia neither support an actively flexing Panama (Silver et al., 1990), nor an active left-lateral shearing (Mann and Corrigan, 1990), though geology suggests that both have been important deformation mechanisms in the geologic past. Seismicity (Marshall et al., 2000) and GPS results confirm a rigid Panama microplate that includes much of Costa Rica, as has been proposed by several authors (Kellogg and Vega, 1995; Lundgren et al., 1999) (Fig. 1). The measured velocities of the sites on the Nazca plate relative to the Panama microplate (Fig. 3) are consistent with left-lateral slip on a fault south of Panama, as proposed by Jordan (1975) and described by Westbrook et al. (1995). The relative velocities of the sites on the Nazca plate (MALS and GALA) are consistent with a single Euler vector for the Nazca plate (Trenkamp and Kellogg, in prep.) and do not require nonrigid behavior of the northern Nazca plate, as was suggested by Wolters (1986) and Adamek et al. (1988), and Kellogg and Vega (1995). The hypothesis of a separate microplate between the Nazca plate and the Panama–Costa Rica microplate defined by motion along Hey's (1977) fault north of Malpelo Island cannot be tested with the available data.

The northeastward displacement vectors for the three sites in southeastern Costa Rica (Fig. 3) are indistinguishable from the vector for David (DAVI) in western Panama. These displacements can be interpreted as the result of the eastward motion of the Panama microplate, plus elastic locking associated with the subduction of the Cocos Ridge. The anomalous Limon (LIMO) displacement may include post-seismic slip from the 1991 earthquake. The two sites in northwest Costa Rica, LIBE and ETCG, are moving in a distinct WNW direction relative to the Panama microplate. We therefore locate the western boundary of the Panama microplate between ETCG and VUEL. This boundary coincides with a seismic zone of left-lateral strike-slip motion recognized by Fan et al. (1993).

4.4. Caribbean plate subduction

The Caribbean plate interacts directly with at least three lithospheric plates: North America, South America, and

Cocos (Fig. 1), and many models have been proposed for Caribbean neotectonics (Jordan, 1975; Ladd, 1976; Burke et al., 1984; Stein et al., 1988; Mann et al., 1990; DeMets et al., 1994; Deng and Sykes, 1995). Of these interactions, one of the most controversial problems in Caribbean tectonics is the location of the Caribbean–South American plate boundary. Several studies of historical seismicity place the southwestern Caribbean–South American boundary along the Bocono fault in the Venezuelan Andes (Dewey, 1972; Aggarwal, 1983). Focal mechanisms along the southeastern Caribbean margin suggest right-lateral transpression with slow abduction of the southern Caribbean plate onto South America (Perez and Aggarwal, 1981; Speed, 1985). Seismic reflection and gravity surveys expose a major folded sedimentary basin south of the Venezuelan and Colombian topographic basins from the Magdalena Delta to the Los Roques Canyon (Edgar et al., 1971; Case, 1974). Multichannel seismic reflection profiles across this south Caribbean deformed belt show that Caribbean acoustic basement has underthrust the deformed belt (Silver et al., 1975; Bowin, 1976; Talwani et al., 1977; Lu and McMillen, 1982; Lehner et al., 1983; Ladd et al., 1984). Folding of the youngest sediments and the presence of a large isostatic negative gravity anomaly over the Curacao Ridge suggest active deformation. Furthermore, Dewey (1972) and Pennington (1981) recognized a zone of earthquakes dipping about 20° to the southeast and terminating 200 km below the Maracaibo Basin. Kellogg and Bonini (1982) and Toto and Kellogg (1992) interpreted these earthquakes as a Benioff zone produced by slow amagmatic subduction of Caribbean lithosphere. This interpretation is supported by seismic tomographic evidence for a south-dipping, high velocity slab (van der Hilst and Mann, 1994), studies of intermediate depth seismicity (Malave and Suarez, 1995), microseismicity (Perez et al., 1997), and the structure of northern and eastern Venezuela (Lallemant, 1997).

CASA GPS measurements show oblique east–southeast convergence of 20 ± 2 mm/a between the Caribbean island San Andres (SANA) and stable South America (Fig. 3). This result is consistent with the angular velocity vector for Caribbean–South American relative motion based on GPS results from eight Caribbean sites and five South American sites (51.5°N, −65.7°E, 0.272°/m.y.) of Weber et al. (2001). Our results and the Weber et al. (2001) velocity vector are also consistent with the GPS results of Perez et al. (2001) for the Caribbean–Venezuelan margin, which indicates east–west dextral displacement of about 20 mm/a. Lateral escape of the North Andes Block to the northeast along the Bocono–East Andes–DGM fault system at 6 ± 2 mm/a increases the southward component of the Caribbean–North Andes relative motion. The relative Caribbean (SANA)–North Andes (BOGO) vector is 14 ± 2 mm/a to the southeast. Southeastward motion at two sites on the North Colombia accretionary prism, Monteria (MONT) and Cartegena (CART), relative to the North Andes (BOGO) suggests elastic deformation produced by Caribbean subduction and Panama–North Andes collision or permanent eastward shear deformation of the South Caribbean deformed belt..

CASA GPS measurements show a 7 ± 2 mm/a southwestward convergence between the Caribbean plate (SANA) and the Panama microplate. This southwest convergence produced the April 1991 Costa Rica earthquake ($M_s = 7.5$) (Goes et al., 1993; Lundgren et al., 1993; Protti and Schwartz, 1994; Suarez et al., 1995), active folding in the north Panama deformed belt (Silver et al., 1995), and a south-dipping Wadati–Benioff zone beneath Panama (Adamek et al., 1988; Protti et al., 1994; Mann and Kolarsky, 1995; Silver et al., 1995).

Pleistocene activity on the Santa Marta–Bucaramanga fault system (Fig. 2) is shown by deformed terraces and offset stream patterns (Campbell, 1968). Although we do not have direct measurements across the Santa Marta–Bucaramanga fault, a relative left-lateral displacement of up to 6 ± 2 mm/a is possible. This estimate is the vector difference between Cartagena (CART) and Valledupar (VDUP) and between Bucaramanga (BUCM) and El Batey (ELBA) parallel to the fault.

5. Summary and conclusions

CASA GPS measurements show that rapid subduction of the Nazca plate is occurring along the length of the Colombia–Ecuador trench. The subduction appears to be accommodated differently from south to north along the trench, probably due to the influence of the subduction of the Carnegie aseismic ridge in Ecuador and southern Colombia. Coastal sites in Ecuador and southern Colombia (MANT, PAJA, MUIS, ESME, and TUMA) show significant transfer of the motion of the subducting slab to the overriding plate and are characterized by large eastward components to their relative motion vectors. These vectors are hypothesized to reflect two modes of deformation, elastic recoverable strain and active faulting associated with permanent shortening, and suggest a possible rationale for the repeat sequences of great earthquakes. Sites in central western Colombia (BUEN and BHSL) have a minimal eastern component to their vectors and have not historically experienced great earthquakes.

Convergence rates along the Colombia–Ecuador trench and the transferred motion to the North Andes, escaping rigidly at 6 ± 2 mm/a to the northeast, support the inference that present plate velocities have slowed relative to time-averaged plate motions (Norabuena et al., 1999). The observed permanent Andean shortening normal to the margin and consistent northeastward escape of the northern Andes parallel to the margin for more than 1400 km from Ecuador to Venezuela suggests that either the margin parallel strength of the North Andes is much greater than its margin normal strength or, more likely, that the South

American craton is acting as a rigid buttress. The GPS measurements to date are insufficient to demonstrate distinct North Andes and Maracaibo Blocks, as proposed by Mann and Burke (1984). The measurements are consistent, however, with possible left-lateral slip on the Santa Marta–Bucaramanga fault.

In northwestern Colombia and Panama, CASA measurements demonstrate the active collision of Panama with Colombia and ongoing deformation up to 550 km from the suture zone. Velocity vectors within Panama suggest that the Panama microplate is behaving as an approximately rigid indenter. Combined with the work of Lundgren et al. (1999) and Marshall et al. (2000), CASA GPS results confirm a rigid Panama microplate whose western boundary is in central Costa Rica. The velocities of the two vectors on the Nazca plate (GALA and MALS) relative to the Panama microplate are consistent with left-lateral slip on a fault south of Panama and do not require a separate north Nazca microplate. The Caribbean–South American convergence rate is 20 ± 2 mm/a.

Various driving mechanisms have been proposed for the northeastward escape of the North Andes. Pindell and Dewey (1982) proposed that the Panama collision is driving North Andean/Maracaibo escape. This mechanism is unlikely to be significant in Ecuador and southern Colombia, however. Russo and Silver (1995), based on evidence of seismic shear wave splitting, suggested that mantle flow from the Pacific into the Caribbean is interacting with subducting mantle slabs. According to Pennington (1981) and Gutscher et al. (1999), the arrival of the Carnegie Ridge at the Ecuador trench (Fig. 1) initiated the escape of the North Andes. Kellogg and Mohriak (2001) proposed that the rapid oblique subduction of the Nazca plate, as well as the Carnegie Ridge, may drive the North Andean detachment. McCaffrey (1994) noted that greater plate obliquities (Sumatra, New Zealand, Aleutians) generally correlate with greater arc-parallel slip partitioning. Geodynamic models are needed to determine whether mantle flow is a potential driving mechanism. Ridge subduction may also be important. The uncoupling of Panama from the Caribbean plate and its eastward collision with the North Andes may have been driven by oblique subduction of the Cocos Ridge and the Nazca and Cocos plates (Mann and Kolarsky, 1995).

Continued GPS measurements are needed to differentiate between permanent deformation and transient visco-elastic deformation of the Andean margin. Site densification will show whether permanent deformation is confined to rigid blocks (abrupt changes in direction and velocity of vectors) or is a smoothly varying continuum. Particularly intriguing is the crustal deformation associated with the subduction of the Carnegie Ridge. For example, preliminary GPS measurements suggest that seismic locking, and therefore seismic hazard, is present in southern Ecuador, an area with no great historic earthquakes.

Acknowledgements

Funding for this project was provided through National Science Foundation grants EAR-8617485 and EAR-8904657 and NASA. The observations described herein were the cooperative efforts of many institutions. We especially recognize the efforts of Dr Adolfo Alarco, INGEOMINAS, and Instituto Geografico Augustin Codazzi in Colombia; Colonel Anibal Salazar and Susana Arciniegas and the Instituto Geografico Militar in Ecuador; Instituto Geografico Tommy Guardia in Panama; Paul Lundgren, JPL, for the Costa Rica data; and Hermann Drewes, Deutsches Geodtisches Forschungsinstitute, for the Venezuela data. We thank Tim Dixon, Paul Mann, Hugh Cowan, and Susan Beck for careful reviews that improved the paper. Many other persons and institutions who contributed to the CASA GPS project are listed in Kellogg et al. (1989). Figures 1–4 created with Generic Mapping Tool (GMT) (Wessel and Smith, 1995).

References

Adamek, S., Frohlich, C., Pennington, W.D., 1988. Seismicity of the Caribbean–Nazca boundary; constraints on microplate tectonics of the Panama region. J. Geophys. Res. 93, 2053–2075.

Aggarwal, Y., 1983. Seismic slip rates and earthquake rupture zones in the southern Caribbean: implications for plate motions and earthquake hazard in this region. Abstracts of the 10th Caribbean Geological Conference, p. 16.

Ammon, C.J., Lay, T., Velasco, A.A., Vidale, J.E., 1994. Routine estimation of earthquake source complexity; the 18 October 1992 Colombian earthquake. Bull. Seismol. Soc. Am. 84, 1266–1271.

Beck Jr, M.E., 1991. Coastwise transport reconsidered, lateral displacements in oblique subduction zones and tectonic consequences. Phys. Earth Planet. Int. 68, 1–8.

Blewitt, G., 2000. Carrier phase ambiguity resolution for the Global Positioning System applied to geodetic baselines up to 2000 km. J. Geophys. Res. 94, 10,187–10,203.

Blewitt, G., 1990. An automatic editing algorithm for GPS data. Geophys. Res. Lett. 17, 199–202.

Bowin, C., 1976. Caribbean gravity field and plate tectonics. Spec. Pap.—Geol. Soc. Am. 169, 79.

Burke, K., Cooper, C., Dewey, J.F., Mann, P., Pindell, J.L., 1984. Caribbean tectonics and relative plate motions. The Caribbean–South American plate boundary and regional tectonics, Bonini, W.E., Hargraves, R.B., Shagam, R. (Eds.). Mem.—Geological Soc. Am. 162, 31–63.

Campbell, C.J., 1968. The Santa Marta wrench fault of Colombia and its regional setting: transactions. Caribbean Geological Conference IV, Trinidad, 1965, pp. 247–260.

Case, J.E., 1974. Major basins along the continental margin of northern South America. In: Burk, C.A., Drake, C.L. (Eds.). The Geology of Continental Margins. pp. 733–741.

Chase, C.G., 1978. Plate kinematics: the Americas, East Africa, and the rest of the world. Earth Planet. Sci. Lett. 37, 355–368.

Colletta, B., Gebrard, F., Letouzey, J., Werner, P., Rudkiewitz, J.L., 1990. Tectonic style and crustal structure of the Eastern Cordillera (Colombia) from a balanced cross-section. Petroleum and Tectonics in Mobile Belts, Letouzey, J.P. (Ed.). Editions Technip, 81–100.

DeMets, C., Gordon, R.G., Argus, D.F., Stein, S., 1990. Current plate motions. Geophys. J. Int. 101, 425–478.

DeMets, C., Gordon, R.G., Argus, D.F., Stein, S., 1994. Effect of recent revisions to the geomagnetic reversal time scale on estimates of current plate motions. Geophys. Res. Lett. 21, 2191–2194.

Deng, J., Sykes, L.R., 1995. Determination of Euler Pole for contemporary relative motion of Caribbean and North American plates using slip vectors of interplate earthquakes. Tectonics 14, 39–53.

Dewey, J.W., 1972. Seismicity and tectonics of western Venezuela. Bull. Seismol. Soc. Am. 62, 1711–1751.

Dewey, J.F., Bird, J.M., 1970. Mountain belts and the new global tectonics. J. Geophys. Res. 75, 2625–2647.

Duque-Caro, H., 1990. The Choco Block in the northwestern corner of South America; structural, tectonostratigraphic, and paleogeographic implications. J. South Am. Earth Sci. 3, 71–84.

Edgar, N.T., Ewing, J.I., Hennion, J., 1971. Seismic refraction and reflection in Caribbean sea. Am. Assoc. Petrol. Geol. Bull. 55, 833–870.

Ego, F., Sebrier, M., Lavenu, A., Yepes, H., Egues, A., 1996. Quaternary state of stress in the Northern Andes and the restraining bend model for the Ecuadorian Andes. Geodynamics of the Andes, Dewey, J.F., Lamb, S.H. (Eds.). Tectonophysics 259, 101–116.

Fan, G., Beck, S.L., Wallace, T.C., 1993. The seismic source parameters of the 1991 Costa Rica aftershock sequence: evidence for a transcurrent plate boundary. J. Geophys. Res. 98, 15759–15778.

Freymueller, J.T., 1991. CASA—Central and South America GPS geodesy: Crustal motions determined from 1988 and 1990 epoch measurements in Colombia, Costa Rica and Ecuador. PhD Dissertation. University of South Carolina, Columbia, pp. 172.

Freymueller, J.T., Kellogg, J.N., Vega, V., 1993. Plate motions in the North Andean Region. J. Geophys. Res. 98, 21853–21863.

Goes, S.D.B., Velasco, A.A., Schwartz, S.Y., Lay, T., 1993. The April 22, 1991, Valle de la Estrella, Costa Rica ($M_w = 7.7$) earthquake and its tectonic implications; a broadband seismic study. J. Geophys. Res. 98, 8127–8142.

Gomberg, J., Ellis, M., 1994. Topography and tectonics of the central New Madrid seismic zone. J. Geophys. Res. 99 (20), 20,299–20,310.

Gutscher, M.A., Malavieille, J., Lallemand, S., Collot, J.Y., 1999. Tectonic segmentation of the North Andean margin; impact of the Carnegie Ridge collision. Earth Planet. Sci. Lett. 168, 255–270.

Heflin, M., Beriger, W., Blewitt, G., Freedman, A.P., Hurst, K., Lichten, S., Lindqwister, U.J., Vigue, Y., Webb, F., Yunck, T.P., Zumberge, J., 1992. Global geodesy using GPS without fiducial sites. Geophys. Res. Lett. 19, 131–134.

Henneberg, H.G., 1983. Geodetic control of neotectonics in Venezuela. Tectonophysics 97, 1–15.

Hey, R., 1977. Tectonic evolution of the Cocos–Nazca spreading center. Geol. Soc. Am. Bull. 88, 1404–1420.

van der Hilst, R., Mann, P., 1994. Tectonic implications of tomographic images of subducted lithosphere beneath northwestern South America. Geology (Boulder) 22, 451–454.

Hutchings, L., Turcotte, T., McBride, J., 1981. Microseismicity along the Dolores shear zone in Antioquia, Colombia. Earthquake notes 52, 68–69.

Isaacs, B., Oliver, J., Sykes, L.R., 1968. Seismology and the new global tectonics. J. Geophys. Res. 73, 5855–5899.

Jarrard, R.D., 1986. Terrane motion by strike-slip faulting of forearc slivers. Geology (Boulder) 14, 780–783.

Jordan, T., 1975. The present day motions of the Caribbean plate. J. Geophys. Res. 80, 4433–4439.

Kanamori, H., 1983. Magnitude scale and quantification of earthquakes. Tectonophysics 93, 185–199.

Kanamori, H., McNally, K.C., 1982. Variable rupture mode of the subduction zone along the Ecuador–Colombia coast. Bull. Seismol. Soc. Am. 72, 1241–1253.

Keigwin, L.D., 1978. Pliocene closing of the Isthmus of Panama, based on biostratigraphic evidence from nearby Pacific Ocean and Caribbean Sea cores. Geology (Boulder) 6, 630–634.

Keigwin, L., 1982. Isotopic paleoceanography of the Caribbean and East Pacific; role of Panama Uplift in late Neogene time. Science 217, 350–353.

Kelleher, J.A., 1972. Rupture zones of large South American earthquakes and some predictions. J. Geophys. Res. 77, 2087–2103.

Keller, G., Zenker, C.E., Stone, S.M., 1989. Late Neogene history of the Pacific–Caribbean gateway. J. South Am. Earth Sci. 2, 73–108.

Kellogg, J.N., Bonini, W.E., 1982. Subduction of the Caribbean Plate and basement uplifts in the overriding South American Plate. Tectonics 1, 251–276.

Kellogg, J., Mohriak, W., 2001. Tectonic and geological environment of coastal South America. In: Seeliger, U., Kjerfve, B. (Eds.). Ecological Studies. Coastal Marine Ecosystems of Latin America, vol. 144. Springer, Berlin, pp. 1–16.

Kellogg, J.N., Vega, V., 1995. Tectonic development of Panama, Costa Rica, and the Colombian Andes: constraints from global positioning system geodetic studies and gravity. In: Mann, P. (Ed.). Geologic and Tectonic Development of the Caribbean plate Boundary in Southern Central America. GSA Special Paper, 295. pp. 75–90.

Kellogg, J.N., Ogujiofor, I.J., Kansaka, D.R., 1985. Cenozoic tectonics of the Panama and North Andes blocks. Memorias—Congreso Latinoamericano de Geologia 6, 34–49.

Kellogg, J.N., Dixon, T.H., Neilan, R.E., 1989. CASA; Central and South America GPS geodesy. Eos, Trans. AGU 70, 649–651 655–656.

Ladd, J.W., 1976. Relative motion of South America with respect to North America and Caribbean tectonics. Geol. Soc. Am. Bull. 87, 969–976.

Ladd, J.W., Truchan, M., Talwani, M., Stoffa, P.L., Buhl, P., Houtz, R., Mauffret, A., Westbrook, G.K., 1984. Seismic reflection profiles across the southern margin of the Caribbean. The Caribbean–South American plate boundary and regional tectonics, Bonini, W.E., Hargraves, R.B., Shagam, R. (Eds.). Mem.—Geol. Soc. Am., 153–159.

Lallemant, H.G.A., 1997. Transpression, displacement partitioning, and exhumation in the eastern Caribbean/South American plate boundary zone. Tectonics 16, 272–289.

Lavenu, A., Winter, T., Davila, F., 1995. A Pliocene–Quaternary compressional basin in the Interandean Depression, central Ecuador. Geophys. J. Int. 121, 279–300.

Leffler, L., Stein, S., Mao, A., Dixon, T., Ellis, M.A., Ocala, L., Selwyn, S.J., 1997. Constraints on present-day shortening rate across the Central eastern Andes from GPS data, Geophys. Res. Lett. 24, 1031–1034.

Lehner, P., Doust, H., Bakker, G., Allenbach, P., Gueneau, J., 1983. Active margins; Caribbean margin of South America, profiles C-1422, C-1412, and C-1413. In: Bally, A.W. (Ed.). Seismic Expression of Structural Styles; a Picture and Work Atlas. AAPG Studies in Geology, vol. 3. p. 15 see also pp. 3.4.2-111–3.4.2-128.

Le Pichon, X., 1968. Sea-floor spreading and continental drift. J. Geophys. Res. 73, 3661–3697.

Li, Y., Toksoz, M.N., 1993. Study of the source process of the 1992 Colombia $M_s = 7.3$ earthquake with the empirical Green's function method. Geophys. Res. Lett. 20, 1087–1090.

Lichten, S.M., Border, J.S., 1987. Strategies for high-precision global positioning system orbit determination. J. Geophys. Res. 92, 12,751–12,762.

Lonsdale, P., Klitgord, K.D., 1978. Structure and tectonic history of the eastern Panama Basin. Geol. Soc. Am. Bull. 89, 981–999.

Lu, R.S., McMillen, K.J., 1982. Multichannel seismic survey of the Colombia Basin and adjacent margins. Studies in Continental Margin Geology, Watkins, J.S., Drake, C.L. (Eds.). AAPG Mem. 34, 395–410.

Lundgren, P.R., Wolf, S.K., Protti, M., Hurst, K.J., 1993. GPS measurements of crustal deformation associated with the 22 April 1991, Valle de la Estrella, Costa Rica earthquake. Geophys. Res. Lett. 20, 407–410.

Lundgren, P., Protti, M., Donnellan, A., Heflin, M., Hernandez, E., Jefferson, D., 1999. Seismic cycle and plate margin deformation in Costa Rica; GPS observations from 1994 to 1997. J. Geophys. Res. 104 (28), 28,915–28,926.

Malave, G., Suarez, G., 1995. Intermediate-depth seismicity in northern Colombia and western Venezuela and its relationship to Caribbean Plate subduction. Tectonics 14, 617–628.

Mann, P., Burke, K., 1984. Neotectonics of the Caribbean. Rev. Geophys. Space Phys. 22, 309–362.

Mann, P., Corrigan, J., 1990. Model for late Neogene deformation in Panama. Geology (Boulder) 18, 558–562.

Mann, P., Kolarsky, R.A., 1995. East Panama deformed belt; structure, age, and neotectonic significance. Geologic and tectonic development of the Caribbean Plate boundary in southern Central America, Mann, P. (Ed.). Spec. Pap.—Geol. Soc. Am. 295, 111–130.

Mann, P., Schubert, C., Burke, K., 1990. Review of Caribbean neotectonics. In: Dengo, G., Case, J.E. (Eds.). The Caribbean region, The Geology of North America. pp. 307–338.

Marshall, J.S., Fisher, D.M., Gardner, T.W., 2000. Central Costa Rica deformed belt: kinematics of diffuse faulting across the western Panama block. Tectonics 19, 468–492.

McCaffrey, R., 1992. Oblique plate convergence, slip vectors and forearc deformation. J. Geophys. Res. 97, 8905–8915.

McCaffrey, R., 1994. Global variability in subduction thrust zone–forearc systems. Pure Appl. Geophys. 142, 173–224.

Meissner, R.O., Flueh, E.R., Stibane, F., Berg, E., 1976. Dynamics of the active plate boundary in Southwest Colombia according to recent geophysical measurements. Tectonophysics 35, 115–136.

Mendoza, C., Dewey, J.W., 1984. Seismicity associated with the great Colombia–Ecuador earthquakes of 1942, 1958, and 1979; implications for barrier models of earthquake rupture. Bull. Seismol. Soc. Am. 74, 577–593.

Minster, J.B., Jordan, T.H., 1978. Present day plate motions. J. Geophys. Res. 83, 5331–5354.

Minster, J.B., Jordan, T.H., Molnar, P., Haines, E., 1974. Numerical modeling of instantaneous plate tectonics. Geophys. J. R. Astr. Soc. 36, 541–576.

Nishenko, S.P., 1989. Circum-Pacific seismic potential 1989–1999. Open-File Report—US Geological Survey, OF 89-0086, p. 126.

Norabuena, E., Leffler-Griffin, L., Mao, A., Dixon, T., Stein, S., Sacks, I., Selwyn, O.L., Ellis, M., 1998. Space geodetic observations of Nazca-South America convergence across the central Andes. Science 279, 358–362.

Norabuena, E.O., Dixon, T.H., Stein, S., Harrison, C.G.A., 1999. Decelerating Nazca–South America and Nazca–Pacific plate motions. Geophys. Res. Lett. 26, 3405–3408.

Papadimitriou, E.E., 1993. Long-term earthquake prediction along the western coast of South and Central America based on a time predictable model. PAGEOPH 140, 301–316.

Pennington, W.D., 1981. Subduction of the eastern Panama Basin and seismotectonics of northwestern South America. J. Geophys. Res. 86, 10753–10770.

Perez, O.J., Aggarwal, Y.P., 1981. Present-day tectonics of the southeastern Caribbean and northeastern Venezuela. J. Geophys. Res. 86, 10791–10804.

Perez, O.J., Jaimes, M.A., Garciacaro, E., 1997. Microseismicity evidence for subduction of the Caribbean Plate beneath the South American Plate in northwestern Venezuela. J. Geophys. Res. 102 (17), 17,875–17,882.

Perez, O.J., Bilham, R., Bendick, R., Velandia, J.R., Hernández, N., Moncayo, C., Hoyer, M., Kozuch, M., 2001. Velocity field across the southern Caribbean plate boundary and estimates of Caribbean/South American plate motion using GPS geodesy 1994–2000. Geophys. Res. Lett. 28, 2987–2990.

Pindell, J.L., Dewey, J.F., 1982. Permo–Triassic reconstruction of western Pangea and the evolution of the Gulf of Mexico/Caribbean region. Tectonics 1, 179–211.

Protti, M., Schwartz, S.Y., 1994. Mechanics of back arc deformation in Costa Rica; evidence from an aftershock study of the April 22, 1991, Valle de la Estrella, Costa Rica, earthquake ($M_w = 7.7$). Tectonics 13, 1093–1107.

Protti, M., Guendel, F., McNally, K., 1994. The geometry of the Wadati–Benioff zone under southern Central America and its tectonic significance; results from a high-resolution local seismographic network. Phys. Earth Planet. Int. 84, 271–287.

Ruff, L.J., 1996. Large earthquakes in subduction zones; segment interaction and recurrence times. In: Bebout, G.E., Scholl, D.W., Kirby, S.H., Platt, J.P. (Eds.). Subduction Top to Bottom. Geophysical Monograph, 96. pp. 91–104.

Russo, R., Silver, P., 1995. The Andes' deep origins. Natural History 2, 53–58.

Savage, J.C., 1983. A dislocation model of strain accumulation and release at a subduction zone. J. Geophys. Res. 88, 4984–4996.

Schubert, C., 1980. Late-Cenozoic pull-apart basins, Bocono fault zone, Venezuelan Andes. J. Struct. Geol. 2, 463–468.

Schubert, C., 1982. Neotectonics of Bocono Fault, western Venezuela. Tectonophysics 85, 205–220.

Silver, E.A., Case, J.E., MacGillavry, H.J., 1975. Geophysical study of the Venezuelan borderland. Geol. Soc. Am. Bull. 86, 213–226.

Silver, E.A., Reed, D.L., Tagudin, J.E., Heil, D.J., 1990. Implications of the north and south Panama thrust belts for the origin of the Panama Orocline. Tectonics 9, 261–281.

Silver, E.A., Galewsky, J., McIntosh, K.D., 1995. Variation in structure, style, and driving mechanism of adjoining segments of the North Panama deformed belt. Geologic and tectonic development of the Caribbean plate boundary in southern Central America, Mann, P. (Ed.). Spec. Pap.—Geol. Soc. Am. 295, 225–233.

Speed, R.C., 1985. Cenozoic collision of the Lesser Antilles arc and continental South America and the origin of the El Pilar Fault. Tectonics 4, 41–69.

Stein, S., DeMets, C., Gordon, R.G., Brodholt, J., Argus, D., Engelin, J.F., Lundgren, P., Stein, C., Wiens, D.A., Woods, D.F., 1988. A test of alternative Caribbean Plate relative motion models. J. Geophys. Res. 93, 3041–3050.

Suarez, G., Molnar, P., Burchfiel, C.B., 1983. Seismicity, fault plane solutions, depth of faulting, and active tectonics of the Andes of Peru, Ecuador, and southern Colombia. J. Geophys. Res. 88, 10,403–10,428.

Suarez, G., Pardo, M., Dominguez, J., Ponc, L., Montero, W., Boschini, I., Rojas, W., 1995. The Limon, Costa Rica earthquake of April 22, 1991; back arc thrusting and collisional tectonics in a subduction environment. Tectonics 14, 518–530.

Swenson, J.L., Beck, S.L., 1996. Historical 1942 Ecuador and 1942 Peru subduction earthquakes, and earthquake cycles along Colombia–Ecuador and Peru subduction segments. PAGEOPH 146, 67–101.

Talwani, M., Windisch, C.C., Stoffa, P.L., Buhl, P., Houtz, R.E., 1977. Multichannel seismic study in the Venezuelan Basin and the Curacao Ridge. In: Talwani, M., Pitman III, W.C. (Eds.). Island Arcs, Deep Sea Trenches and Back-Arc Basins. Maurice Ewing Series, vol. 1. pp. 83–98.

Thatcher, W., 1995. Microplate versus continuum descriptions of active tectonic deformation. J. Geophys. Res. 100, 3885–3894.

Tibaldi, A., Leon, J.R., 2000. Morphometry of late Pleistocene–Holocene faulting and volcanotectonic relationship in the southern Andes of Colombia. Tectonics 19, 358–377.

Tichelaar, B.W., Ruff, L.J., 1991. Seismic coupling along the Chilean subduction zone. J. Geophys. Res. 96, 11,997–12,022.

Toto, El.A., Kellogg, J.N., 1992. Structure of the Sinu-San Jacinto fold belt; an active accretionary prism in northern Colombia. J. South Am. Earth Sci. 5, 211–222.

Wadge, G., Burke, K., 1983. Neogene Caribbean plate rotation and associated Central American tectonic evolution. Tectonics 2, 633–643.

Wallace, T.C., Beck, S.L., 1993. The Oct. 17–18, 1992 Colombian earthquakes; slip partitioning or faulting complexity. Seismol. Res. Lett. 64, 29.

Weber, J.C., Dixon, T.H., DeMets, C., Ambeh, W.B., Jansma, P., Mattioli, G., Saleh, J., Sella, G., Bilham, R., Pérez, O., 2001. GPS estimate of relative motion between the Caribbean and South American plates, and geological implications for Trinidad and Venezuela. Geology 29, 75–78.

Wessel, P., Smith, W.H.T., 1995. New version of the generic mapping tools released. EOS Trans. Am. Geophys. U. 76, 329.

Westbrook, G.K., Hardy, N.C., Heath, R.P., 1995. Structure and tectonics of the Panama–Nazca plate boundary. In: Mann, P. (Ed.). Geologic and Tectonic Development of the Caribbean Plate Boundary in Southern Central America. GSA Special Paper, 295. pp. 91–109.

Winter, T., Avouac, J.-P., Lavenu, A., 1993. Late Quaternary kinematics of the Pallatanga strike-slip fault (central Ecuador) from topographic measurements of displaced morphological features. Geophys. J. Int. 115 (3), 905–920.

Wolters, B., 1986. Seismicity and tectonics of southern Central America and adjacent regions with special attention to the surroundings of Panama. Tectonophysics 128, 21–46.